Available online at www.sciencedirect.com
SCIENCE DIRECT®
Biochimica et Biophysica Acta 1748 (2005) 174–179
BIOCHIMICA ET BIOPHYSICA ACTA
BBA
http://www.elsevier.com/locate/bba

Comparative analysis of the cytotoxicity of homopolymeric amino acids

Yoko Oma, Yoshihiro Kino, Noboru Sasagawa, Shoichi Ishiura*

Department of Life Sciences, Graduate School of Arts and Sciences, The University of Tokyo, Japan

Received 8 November 2004; received in revised form 28 December 2004; accepted 29 December 2004
Available online 27 January 2005

Abstract

Many human proteins have homopolymeric amino acid (HPAA) tracts, although the physiological significance or cellular effects of their presence is poorly understood. We previously reported that 20 kinds of HPAAs show characteristic intracellular localization and that among those, hydrophobic HPAAs aggregate strongly and form high molecular weight proteins when expressed in cultured cells. In this study, we investigated the cytotoxicity of 20 kinds of HPAAs. HPAA tracts of ~30 residues fused to the C-terminus of YFP were expressed in COS-7 cells. Cells expressing homopolymeric-Cys, -Ile, -Leu, and -Val showed low viability in Trypan Blue assay. Caspase-3 activity, which is usually upregulated in dying cells, was determined by measuring the cleavage of the peptide substrate Ac–DEVD–MCA and by detecting the cleaved active form of the caspase-3 by Western blotting. The activity of caspase-3 was drastically elevated in cells expressing those HPAAs which showed low viability in Trypan Blue assay. Interestingly, it was found that there is a correlation between the hydrophobicity of a single amino acid and the cytotoxicity of the corresponding HPAA as a homopolymer. These results indicate that the hydrophobicity of HPAAs may cause cytotoxicity.

Keywords: Polyglutamine; Polyalanine; Triplet repeat; Cell death; Cytotoxicity; Caspase

1. Introduction

Higher organisms contain thousands of protein species, whose functional diversity is based on the diversity of their components, amino acids, and their numerous combinations. Homopolymeric amino acids (HPAAs) are distinct tracts of amino acids comprising consecutive sequences of the same amino acid, some of which are often found in natural proteins [1]; HPAA tracts may either play some roles in or have effect on cells. Each HPAA has characteristic properties reflecting the diversity of amino acids. Indeed, we recently reported differential patterns of intracellular localization of HPAAs fused to YFP [2]. Moreover, several genetic diseases associated with the expansion of HPAA tracts have been reported [3–6]. Polyglutamine expansions cause several genetically inherited diseases including Huntington's disease. It has been observed that expanded polyglutamine forms neuronal intranuclear inclusions in animal models of polyglutamine diseases and in the central nervous system of patients with these diseases [7,8]. Expanded polyglutamine is thought to confer toxic properties on the disease proteins with a dominant gain-of-function that causes cell death or dysfunction. However, the role of the aggregate formation in disease pathology is not clarified yet [9–11]. Besides expanded polyglutamine, intranuclear aggregation of the causative protein with expanded polyalanine in skeletal muscle fibers is the morphological hallmark of oculopharyngeal muscular dystrophy (OPMD), one of the polyalanine diseases [12,13], suggesting a possible common mechanism between OPMD and polyglutamine diseases. Huntington's disease-like 2, a novel disease with similar symptoms to Huntington's disease, has been described as being caused by the expansion of CTG repeats, which are translated into either polyalanine or polyleucine stretches [14].

Even outside a disease-related protein context, polyglutamine or polyalanine tracts themselves have been

* Corresponding author. Fax: +81 3 5454 6739.
E-mail address: cishiura@mail.ecc.u-tokyo.ac.jp (S. Ishiura).

1570-9639/$ - see front matter © 2005 Elsevier B.V. All rights reserved.
doi:10.1016/j.bbapap.2004.12.017

studied and their expansion has been shown to confer aggregative and cytotoxic properties. For example, when GFP-fused polyglutamine tracts of 19, 35, 56, and 80 residues were expressed in primary neurons, 35, 56, and 80 residues formed aggregate(s) and 80 residues upregulated caspase activity [15]. Similarly, the expression of GFP-fused polyalanine tracts of 19, and 37 residues in COS-7 cells results in formation of aggregates with higher rates of cell death for cells containing the 19 or 37 residue constructs compared with cells containing the 0 or 7 residue constructs [16]. COS-7 cells, which we used in this study, are often used as a good cellular model of polyglutamine and polyalanine diseases since they mimic many of features of the diseases including length dependent aggregation and cell death. Polyalanine peptides 14 residues in length have been shown to form beta-sheets in vitro [17], and extended polyglutamine repeats have also been shown to form such structures in vitro and in vivo [18,19]. Apart from polyglutamine and polyalanine, polyleucine tracts of 291 residues in length have been reported to possess even stronger cytotoxicity compared to polyglutamine tracts of the same length [20]. These results suggest that the length and species of homopolymeric amino acids may produce varying cytotoxic effects.

To understand the properties of HPAAs comparatively, we previously reported the specific localizations of 20 kinds of HPAAs, and showed that hydrophobic HPAAs aggregate strongly and form high molecular weight complexes [2]. Though intracellular aggregation is limited in polyglutamine and polyalanine diseases, as mentioned above, some HPAAs other than polyglutamine or polyalanine might have cytotoxic effects. In this report, we compared the cytotoxicity of 20 kinds of HPAAs composed of 30 residues under the same experimental conditions.

2. Materials and methods

2.1. Fluorescence microscopy analysis

COS-7 cells were grown in DMEM with 10% fetal bovine serum (Sigma-Aldrich, Tokyo, Japan). Transient transfection was performed using FuGENE 6 Transfection reagent (Roche Diagnostics, Tokyo, Japan) following the manufacturer's instructions. The cells were treated with Hoechst33342 (Sigma-Aldrich, Tokyo, Japan) at 37 °C for 30 min, and the medium was removed and replaced with PBS. The fluorescence of YFP was visualized by fluorescence microscopy IX70 (Olympus, Tokyo, Japan).

2.2. Transfection efficiency

COS-7 cells were transiently transfected with the YFP–HPAA plasmid. After incubation for 48 h, the cells were harvested and dissolved in PBS. The percentage of transfected cells was determined as fluorescent positive cells by flow cytometry (EPICS® XL™, Beckman Coulter).

2.3. Trypan Blue assay

COS-7 cells were seeded at 1.2×10^4 per well in 24-well plates and were transiently transfected with 0.3 μg of YFP–HPAA plasmid after incubation for 19 h. The cells were harvested and treated with Trypan Blue (Sigma-Aldrich, Tokyo, Japan) 48 h after transfection. In each experiment, about 150 cells were examined under a microscope to determine the number of dead cells (stained) and living cells (unstained).

2.4. Caspase-3 assay

COS-7 cells were seeded at 2.0×10^5 per 35 mm dish and were transiently transfected with 0.75 μg of YFP–HPAA plasmids after incubation for 24 h. The cells were harvested and dissolved in extraction buffer (50 mM Tris–HCl, pH7.5, 10 mM 2-mercaptoethanol, 1 mM EDTA) 48 hours after transfection. The samples were subjected to three rounds of freezing in liquid nitrogen for 60 s and thawing in a 30 °C water bath for 90 s, after which the samples were centrifuged at 10,000 ×*g* for 5 min. The total protein (7.4 μg) in the supernatant was dissolved in 200 μl of assay buffer (25 mM Tris–HCl, pH7.5, 10 mM 2-mercaptoethanol, 1 mM EDTA). A fluorescent substrate for caspase-3, Ac-Asp-Glu-Val-Asp-MCA (Peptide Institute, Tokyo, Japan), was added to a final concentration of 5 μM, and the mixtures were incubated at 37 °C for 30 min. The reactions were stopped by the addition of 100 μl of 10% SDS, 1 ml of 0.1 M NaOAc, and the fluorescence was measured with a JASCO FP-777 fluorescence spectrometer (excitation, 380 nm; emission, 460 nm).

2.5. Western blot analysis

COS-7 cells were seeded at 1.5×10^5 per 60 mm dish and were transiently transfected with 2.0 μg of YFP–HPAA plasmids after incubation for 24 h. After incubation for 48 h, the cells were harvested and sonicated in PBS with 1% Triton X-100 and 0.1% protease inhibitor mix (Wako, Osaka, Japan). The protein concentration was measured with a DC protein Assay Kit (Bio-Rad laboratories, Tokyo, Japan). Equal amounts of protein, 41 μg for each sample, were subjected to SDS-polyacrylamide gel electrophoresis on 15% gels and transferred onto PVDF membranes (Finetrap NT-32; Nihon Eido, Tokyo, Japan). The membranes were incubated with Caspase 3 (8G10) rabbit monoclonal antibody (1:1000; Cell Signaling Thechnology, U.S.A.) at 4 °C for overnight, and then with anti-rabbit IgG anitibody at 37 °C for 30 min. The resulting menbranes were visualized with Enhanced

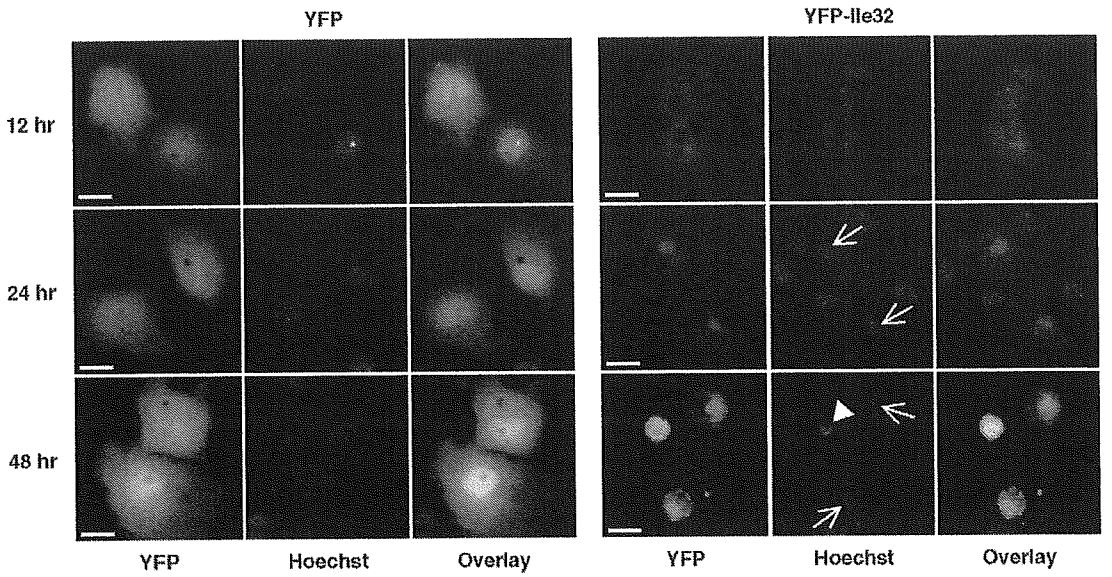

Fig. 1. The intracellular localization of YFP and YFP-fused homopolymeric-Ile32. The nuclei were stained by Hoechst. Homopolymeric-Ile32 formed one large aggregate in the perinuclear region of each cell. The nuclei of the cells expressing homopolymeric-Ile32 showed distorted morphology around the aggregates (arrow) and become aberrant (arrow head) at 48 h after transfection. Scale bar, 20 μm.

Chemiluminescence kit (Amersham Bioscience, Tokyo, Japan).

3. Results

3.1. Cell viability assay

We have previously shown that hydrophobic HPAAs aggregate strongly in COS-7 cells [2]. Fig. 1 shows the intracellular localization of YFP-fused homopolymeric-Ile32, one of the typical aggregate-forming HPAAs. The nuclei of the cells expressing homopolymeric-Ile32 were stained by Hoechst, and showed distorted morphology around the aggregates (arrow) and became aberrant (arrow-head) at 48 h after transfection. We observed many floating cells expressing Ile32, but not YFP only, suggesting that cell death is caused by the expression of this HPAA.

To study the effects of HPAAs on cells, we performed cell viability assays by staining dead cells with Trypan Blue. Twenty HPAAs, each comprising approximately 30 residues (26~32) fused to the C-terminus of YFP, were expressed in COS-7 cells. Forty-eight hours after transfection, we treated cells with Trypan Blue and determined the ratio of stained (dead) cells to unstained (living) cells. The transfection efficiency was examined and there was no significant difference among all constructs on analysis of variance (ANOVA) tests (data not shown). Compared to cells expressing only YFP, cells expressing YFP-fused homopolymeric-Ile, -Cys, -Val, and -Leu showed significantly low viability followed by cells expressing homopolymeric-Phe, -Trp, -Met, and -Ala (Fig. 2).

3.2. Caspase-3 assay

Caspase-3 activity is known to rise at the very downstream point of apoptotic cell death [21]. Forty-eight hours after transfection we assessed the caspase-3 activity by measuring the cleavage of the peptide substrate Ac-DEVD-MCA. Longer HPAAs (Ala70, Gln150) induced higher caspase-3 activities than their shorter counterparts (Fig. 3A), which is consistent with the previous reports that long

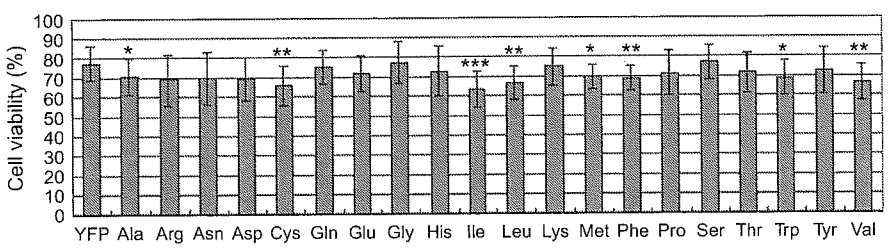

Fig. 2. Cell viability assay. Cell viability was measured 48 h after transfection by Trypan Blue assay. Compared to cells expressing only YFP, cells expressing YFP-fused homopolymeric-Ala, -Cys, -Ile, -Leu, -Met, -Phe, -Trp, and -Val showed low viability. Student's t Test was performed with the control (only YFP). *p<0.05; **p<0.01; ***p<0.001; Mean±S.D.; n=10.

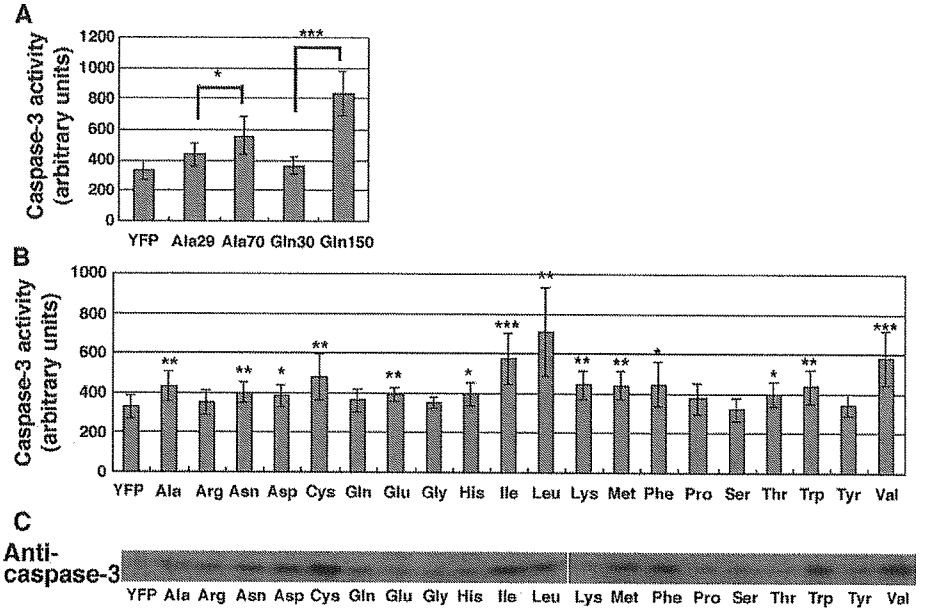

Fig. 3. Caspase-3 assay. Caspase-3 activity was measured 48 h after transfection. (A) Caspase-3 activity was upregulated when longer stretches of polyglutamine (150 residues) or polyalanine (70 residues) were expressed compared to shorter stretches (30 residues). (B) Compared to cells expressing only YFP, cells expressing YFP-fused homopolymeric-Leu, -Val, -Ile, -Cys, followed by -Phe, -Lys and -Met, showed high caspase-3 activities. Student's *t* Test was performed with the control (only YFP). $*p<0.05$; $**p<0.01$; $***p<0.001$; Mean±S.D.; $n=9$ (C) The cleaved active fragment of caspase-3 was detected by Western blot analysis with anti-caspase-3 antibody.

polyglutamine and polyalanine tracts have cytotoxic effects [15,16]. Among the 20 HPAAs comprising 30 residues, a drastic upregulation of caspase-3 occurred in cells expressing homopolymeric-Leu, -Val, -Ile, and -Cys compared with control cells expressing only YFP, suggesting that these HPAAs have strong cytotoxic effects (Fig. 3B). Homopolymeric-Leu produced the highest upregultion of caspase-3, followed by -Val, -Ile, and -Cys. Some other HPAAs, homopolymeric-Ala, -Asn, -Asp, -Glu, -His, -Lys, -Met, -Phe, -Thr, and -Trp, also produced significantly elevated caspase-3 activities. Next, the cleaved active fragment of the caspase-3 (17/19 kDa) was measured by Western blotting with an anti-caspase 3 antibody (Fig. 3C). Cells expressing homopolymeric-Asn, -Asp, -Cys, -Ile, -Leu, -Met, -Phe, -Trp, and -Val showed an increased amount of cleaved active fragment of caspase-3, which is approximately consistent with our caspase-3 assay shown in Fig. 3B. The same experiment was repeated three times and similar results were observed each time (data not shown).

The results of the cell viability assay and the caspase-3 assay declared cytotoxicity of several HPAAs, especially homopolymeric-Cys, -Ile, -Leu and -Val. HPAAs which showed cytotoxicity in these assays seem to be hydrophobic HPAAs. We plotted the cytotoxicity of each HPAA as measured in these experiments, the hydrophobicity of each amino acid [22] versus cell viability and caspase-3 activity

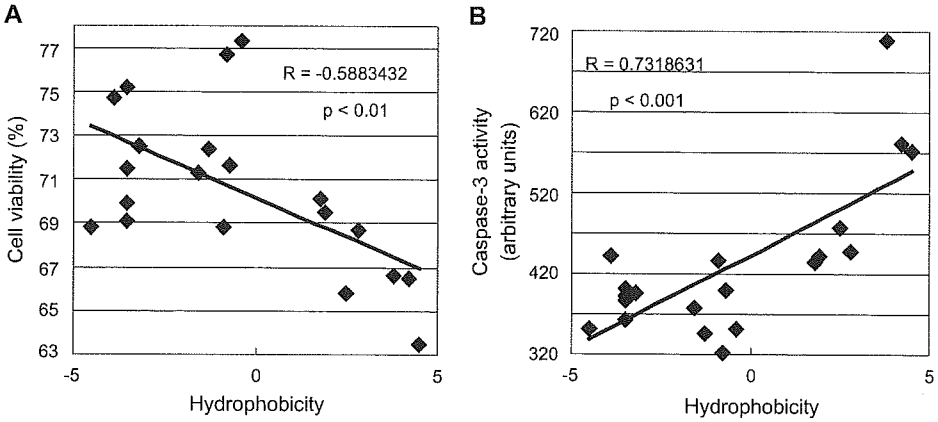

Fig. 4. Cytotoxicity and hydrophobicity. There is a correlation between the level of cytotoxicity of an HPAA and the hydrophobicity of its amino acid. Hydrophobicity of each amino acid as calculated in ref.22 was plotted versus the cytotoxicities of HPAAs measured by (A) the cell viability assay and, (B) the caspase-3 activity assay.

(Fig. 4A and B, respectively). As shown in the plot, there is a significant correlation between the cytotoxicity of an HPAA and the hydrophobicity of its amino acid, indicating that the higher hydrophobic properties of a protein might induce more severe toxicity in cells.

4. Discussion

There are many proteins containing various kinds of HPAAs, and several diseases are caused by the expansions of such amino acid repeats, including polyglutamine and polyalanine. This is the first report which investigated cytotoxicity of not only polyglutamine, polyalanine, or polyleucine but also other HPAAs, all 20 kinds of HPAAs comparatively.

To investigate the effect of all 20 HPAAs in cells, we performed two assays, cell viability assay and caspase-3 activity assay, to detect the cytotoxicity of HPAAs expressed in cells. Our results suggest that among all HPAAs, homopolymeric-Cys and hydrophobic HPAAs such as homopolymeric-Ile, -Leu, and -Val, tend to have highly toxic effects in cells. And there was a correlation between the cytotoxicity of an HPAA and the hydrophobicity of its amino acid, indicating that the higher hydrophobic properties of a protein might induce more severe toxicity in cells. Interestingly, we previously showed that these hydrophobic HPAAs aggregate strongly and form high molecular weight proteins [2]. Therefore, our results suggest that aggregation-prone proteins may have cytotoxicity. Importantly, there is a bias in the distribution of HPAA species, so that hydrophobic HPAAs are rare in natural proteins. In the previous report, we predicted that the scarcity of these HPAAs might derive from their cytotoxicity since those HPAAs aggregate strongly in cells. In this report, we demonstrated the plausibleness of the prediction that HPAAs which aggregate in cells have cytotoxicic effect and might be less abundant in natural proteins. Fig. 5 depicts a diagram of 20 amino acids situated according to their properties with the red circle showing cytotoxicity as revealed in our study. Aliphatic hydrophobic HPAAs and homopolymeric-Cys showed the most significant toxicity in our assays.

The accumulation of altered proteins is a common pathogenic mechanism in several neurodegenerative disorders including polyglutamine diseases, Alzheimer's disease, and Parkinson's disease [9,23]. Although there must be specific mechanisms for each disease according to the responsible protein, aggregate formation itself might have significant relation with toxicity [24]. It has been suggested that the soluble oligomers of these proteins are crucial to the toxic mechanism rather than the subsequent aggregates or fibrils [25]. The role of aggregation or oligomerization is a very important issue for solving the mechanism of the cytoxicity of these proteins. It has been reported that protein aggregation directly impairs the function of the ubiquitin–proteasome system [26] or causes an unfolded protein

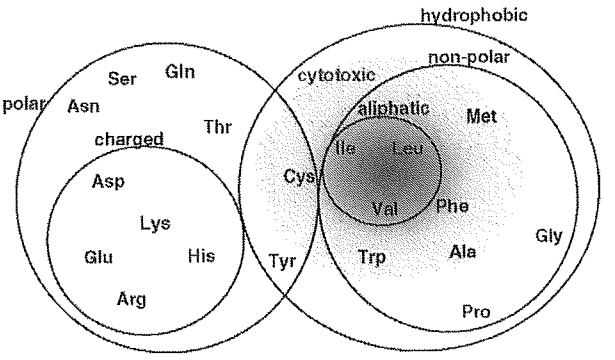

Fig. 5. Properties of single amino acids and the cytotoxicity of their homopolymers. The diagram shows the relationship among 20 amino acids in terms of their properties. Cytotoxic HPAAs are within the red circle.

response [27]. Recently, it has also been reported that endoplasmic reticulum (ER) stress is caused by the accumulation of unfolded and malfolded proteins, including amyloid beta peptide in Alzheimer's diseases [28], polyglutamine-containing proteins [29,30] and prion protein [31].

Here, we show the cytotoxicities of hydrophobic HPAAs in cultured cells, thus confirmed the previous prediction that hydrophobicity of HPAAs might be an important determinant of cytotoxicity as well as aggregation. Furthermore, our system using various kinds of HPAAs not only reveals the specific properties of each HPAA, but also can be used as a model of aggregation-prone proteins with various levels of solubility to clarify the mechanism of aggregation and toxicity.

Acknowledgements

This work was supported in part by a Grant-in-Aid for Scientific Research on Priority Areas—Advanced Brain Science Project—from the Ministry of Education, Culture, Sports, Science and Technology, Japan, and by research grants from the Ministry of Health, Labor, and Welfare, Japan.

References

[1] M.M. Alba, R. Guigo, Comparative analysis of amino acid repeats in rodents and humans, Genome Res. 14 (2004) 549–554.
[2] Y. Oma, Y. Kino, N. Sasagawa, S. Ishiura, Intracellular localization of homopolymeric amino acid-containing protein expressed in mammalian cells, J. Biol. Chem. 279 (2004) 21217–21222.
[3] H.Y. Zoghbi, H.T. Orr, Glutamine repeats and neurodegeneration, Annu. Rev. Neurosci. 23 (2000) 217–247.
[4] R.L. Margolis, C.A. Ross, Expansion explosion: new clues to the pathogenesis of repeat expansion neurodegenerative diseases, Trends Mol. Med. 7 (2001) 479–482.
[5] L.Y. Brown, S.A. Brown, Alanine tracts: the expanding story of human illness and trinucleotide repeats, Trends Genet. 20 (2004) 51–58.
[6] J. Amiel, D. Trochet, M. Clement-Ziza, A. Munnich, S. Lyonnet, Polyalanine expansions in human, Hum. Mol. Genet. 13 (Suppl. 2) (2004) R235–R243.

[7] S.W. Davies, M. Turmaine, B.A. Cozens, M. DiFiglia, A.H. Sharp, C.A. Ross, E. Scherzinger, E.E. Wanker, L. Mangiarini, G.P. Bates, Formation of neuronal intranuclear inclusions underlies the neurological dysfunction in mice transgenic for the HD mutation, Cell 90 (1997) 537–548.
[8] M. DiFiglia, E. Sapp, K.O. Chase, S.W. Davies, G.P. Bates, J.P. Vonsattel, N. Aronin, Aggregation of huntingtin in neuronal intranuclear inclusions and dystrophic neurites in brain, Science 277 (1997) 1990–1993.
[9] M.Y. Sherman, A.L. Goldberg, Cellular defenses against unfolded proteins: a cell biologist thinks about neurodegenerative diseases, Neuron 29 (2001) 15–32.
[10] C.A. Ross, Polyglutamine pathogenesis: emergence of unifying mechanisms for Huntington's disease and related disorders, Neuron 35 (2002) 819–822.
[11] A. Michalik, C. Van Broeckhoven, Pathogenesis of polyglutamine disorders: aggregation revisited, Hum. Mol. Genet. 12 (Spec. No. 2) (2003) R173–R186.
[12] V. Shanmugam, P. Dion, D. Rochefort, J. Laganiere, B. Brais, G.A. Rouleau, PABP2 polyalanine tract expansion causes intranuclear inclusions in oculopharyngeal muscular dystrophy, Ann. Neurol. 48 (2000) 798–802.
[13] M.W. Becher, J.A. Kotzuk, L.E. Davis, D.G. Bear, Intranuclear inclusions in oculopharyngeal muscular dystrophy contain poly(A) binding protein 2, Ann. Neurol. 48 (2000) 812–815.
[14] S.E. Holmes, E. O'Hearn, A. Rosenblatt, C. Callahan, H.S. Hwang, R.G. Ingersoll-Ashworth, A. Fleisher, G. Stevanin, A. Brice, N.T. Potter, C.A. Ross, R.L. Margolis, A repeat expansion in the gene encoding junctophilin-3 is associated with Huntington disease-like 2, Nat. Genet. 29 (2001) 377–378 Erratum in: Nat. Genet. 30 (2002) 123.
[15] K.L. Moulder, O. Onodera, J.R. Burke, W.J. Strittmatter, E.M. Johnson Jr., Generation of neuronal intranuclear inclusions by polyglutamine-GFP: analysis of inclusion clearance and toxicity as a function of polyglutamine length, J. Neurosci. 19 (1999) 705–715.
[16] J. Rankin, A. Wyttenbach, D.C. Rubinsztein, Intracellular green fluorescent protein–polyalanine aggregates are associated with cell death, Biochem. J. 348 (2000) 15–19.
[17] S.E. Blondelle, B. Forood, R.A. Houghten, E. Perez-Paya, Polyalanine-based peptides as models for self-associated beta-pleated-sheet complexes, Biochemistry 36 (1997) 8393–8400.
[18] E. Scherzinger, R. Lurz, M. Turmaine, L. Mangiarini, B. Hollenbach, R. Hasenbank, G.P. Bates, S.W. Davies, H. Lehrach, E.E. Wanker, Huntingtin-encoded polyglutamine expansions form amyloid-like protein aggregates in vitro and in vivo, Cell 90 (1997) 549–558.
[19] C.C. Huang, P.W. Faber, F. Persichetti, V. Mittal, J.P. Vonsattel, M.E. MacDonald, J.F. Gusella, Amyloid formation by mutant huntingtin: threshold, progressivity and recruitment of normal polyglutamine proteins, Somat. Cell Mol. Genet. 24 (1998) 217–233.
[20] J.C. Dorsman, B. Pepers, D. Langenberg, H. Kerkdijk, M. Ijszenga, J.T. den Dunnen, R.A. Roos, G.J. van Ommen, Strong aggregation and increased toxicity of polyleucine over polyglutamine stretches in mammalian cells, Hum. Mol. Genet. 11 (2002) 1487–1496.
[21] E.A. Slee, C. Adrain, S.J. Martin, Serial killers: ordering caspase activation events in apoptosis, Cell Death Differ. 6 (1999) 1067–1074.
[22] J. Kyte, R.F. Doolittle, A simple method for displaying the hydropathic character of a protein, J. Mol. Biol. 157 (1982) 105–132.
[23] J.P. Taylor, J. Hardy, K.H. Fischbeck, Toxic protein in neurodegenerative disease, Science 296 (2002) 1991–1995.
[24] M. Bucciantini, E. Giannoni, F. Chiti, F. Baroni, L. Formigli, J. Zurdo, N. Taddei, G. Ramponi, C.M. Dobson, M. Stefani, Inherent toxicity of aggregates implies a common mechanism for protein misfolding diseases, Nature 416 (2002) 507–511.
[25] R. Kayed, E. Head, J.L. Thompson, T.M. McIntire, S.C. Milton, C.W. Cotman, C.G. Glabe, Common structure of soluble amyloid oligomers implies common mechanism of pathogenesis, Science 300 (2003) 486–489.
[26] N.F. Bence, R.M. Sampat, R.R. Kopito, Impairment of the ubiquitin–proteasome system by protein aggregation, Science 292 (2001) 1552–1555.
[27] M.S. Forman, V.M. Lee, J.Q. Trojanowski, 'Unfolding' pathways in neurodegenerative disease, Trends Neurosci. 26 (2003) 407–410.
[28] T. Nakagawa, H. Zhu, N. Morishima, E. Li, J. Xu, B.A. Yankner, J. Yuan, Caspase-12 mediates endoplasmic-reticulum-specific apoptosis and cytotoxicity by amyloid-beta, Nature 403 (2000) 98–103.
[29] Y. Kouroku, E. Fujita, A. Jimbo, T. Kikuchi, T. Yamagata, M.Y. Momoi, E. Kominami, K. Kuida, K. Sakamaki, S. Yonehara, T. Momoi, Polyglutamine aggregates stimulate ER stress signals and caspase-12 activation, Hum. Mol. Genet. 11 (2002) 1505–1515.
[30] H. Nishitoh, A. Matsuzawa, K. Tobiume, K. Saegusa, K. Takeda, K. Inoue, S. Hori, A. Kakizuka, H. Ichijo, ASK1 is essential for endoplasmic reticulum stress-induced neuronal cell death triggered by expanded polyglutamine repeats, Genes Dev. 16 (2002) 1345–1355.
[31] C. Hetz, M. Russelakis-Carneiro, K. Maundrell, J. Castilla, C. Soto, Caspase-12 and endoplasmic reticulum stress mediate neurotoxicity of pathological prion protein, EMBO J. 22 (2003) 5435–5445.

J. Biochem. **137**, 00–00 (2005)
DOI: 10.1093/jb/mvi058

Denervation Enhances the Expression of SHPS-1 in Rat Skeletal Muscle

Hiroaki Mitsuhashi[1], Ayumu Yoshikawa[1], Noboru Sasagawa[1], Yukiko Hayashi[2] and Shoichi Ishiura[1,*]

[1]Department of Life Sciences, Graduate School of Arts and Sciences, The University of Tokyo, 3-8-1 Komaba, Meguro-ku, Tokyo 153-8902; and [2]Department of Neuromuscular Research, National Institute of Neuroscience, National Center of Neurology and Psychiatry, Kodaira, Tokyo 187-8502

Received October 8, 2004; accepted February 4, 2005

SHPS-1 (Src homology 2 domain containing protein tyrosine phosphatase substrate 1) is a transmembrane glycoprotein containing three immunoglobulin-like motifs in its extracellular domain and immunoreceptor tyrosine-based inhibitory motifs (ITIM) that interact with SHP-2 (Src homology 2 domain containing protein tyrosine phosphatase-2) in its cytoplasmic region. SHPS-1 is highly expressed in brain, but at much lower levels in skeletal muscle. In this study, we found that the level of the SHPS-1 mRNA increases in rat skeletal muscle after denervation. Western blot analysis also confirmed the increase of SHPS-1 in denervated muscle. Moreover, it was found that the glycosylation of SHPS-1 is *N*-linked in a muscle-specific manner, and that this is altered upon innervation or denervation. Immunohistochemistry revealed SHPS-1 immunoreactivity at neuromuscular junctions (NMJs) under innervation, whereas immunoreactivity was observed extrasynaptically in muscle fibers after denervation. Our results indicate that the expression, glycosylation, and localization of SHPS-1 are strongly regulated by the nervous system, and that SHPS-1 may play an important role in denervated skeletal muscle.

Key words: denervation, glycosylation, neuromuscular junction, SHPS-1, skeletal muscle.

Abbreviations: AchRα, acetylcholine receptor α-subunit; ARPP16/19, cAMP-regulated phosphoprotein 16/19; BIT, brain immunoglobulin-like molecule with tyrosine-based activation motifs; α-BTX, α-bungarotoxin; ConA, Concanavalin A; Den, denervation; EDL, extensor digitorum longus; EGF, epidermal growth factor; GAPDH, glyceraldehyde-3-phosphate dehydrogenase; IGF-I, insulin-like growth factor-I; Inn, innervation; MAP kinase, mitogen-activated protein kinase; MFR, macrophage fusion receptor; NCAM, neural cell adhesion molecule; NMJs, neuromuscular junctions; PBS, phosphate-buffered saline; PVDF, polyvinylidene difluoride; SH2, Src homology 2; SHP-1/2, Src homology 2 domain containing protein tyrosine phosphatase-1/2; SHPS-1, Src homology 2 domain containing protein tyrosine phosphatase substrate 1; SIRP, signal-regulatory protein.

The differentiation of skeletal muscle is regulated by the nervous system. Neural innervation sends myotubes into myofibers. Skeletal muscle size, phenotype, and composition are also regulated, in part, by neural factors. Eliminating neural stimuli to muscle *via* peripheral nerve axotomy (denervation) impairs the highly differentiated state of skeletal muscle, leading to muscle atrophy. In addition, denervation results in changes in the expressions of muscle-specific genes, notably myogenic regulatory factors (MRFs) (*1–6*), the type II myosin heavy chain (MHC) isoform (*7*, *8*), and the acetylcholine receptor α subunit (AchRα) (*1*, *6*). For example, AchR is composed of five subunits including the ε-subunit ($\alpha\alpha\beta\delta\varepsilon$), and is restricted to neuromuscular junctions (NMJs) under innervation. But following denervation, the expressions of all AchR subunit genes increase, and the fetal type receptor, including a γ-subunit ($\alpha\alpha\beta\delta\gamma$), localizes throughout the sarcolemma. This implies that skeletal muscle after denervation reverts to a fetal, undifferentiated state both structurally and functionally. The identification and characterization of genes that are activated in denervated muscles might provide clues to the molecular mechanisms of muscle atrophy and differentiation.

SHPS-1 (Src homology 2 domain–containing protein tyrosine phosphatase substrate 1) (*9*), also known as SIRPα (*10*), BIT (*11*), MFR (*12*), and p84 neural adhesion molecule (*13*), is a transmembrane glycoprotein member of the immunoglobulin superfamily. SHPS-1 is abundant in certain neuronal and hematopoietic cells (*13–15*). The tissue distribution of SHPS-1 shows that it is abundant in the brain and spleen, and much less abundant in skeletal muscle (*9*, *16*). SHPS-1 has three immunoglobulin-like domains with multiple *N*-linked glycosylation sites in the extracellular region, and four YXX(L/V/I) motifs, which are putative tyrosine phosphorylation sites and binding sites for the Src homology 2 (SH2) domains of the protein-tyrosine phosphatases SHP-2 and SHP-1 (*9*, *10*), in the cytoplasmic region. Since the binding of SHP-2 to the tyrosine-phosphorylated cytoplasmic domain of SHPS-1 increases the protein tyrosine phosphatase activity of SHP-2 *in vitro* (*11*, *17*), it is thought that SHPS-1 regulates intracellular signaling by recruiting and activating SHP-2 near the plasma membrane. For example, overexpression of SIRPα1, the human homolog of SHPS-1, inhibits the insulin- or EGF-induced activation of MAP kinases and cell growth (*18*). Furthermore,

*To whom correspondence should be addressed. Tel/Fax: +81-3-5454-6739, E-mail: cishiura@mail.ecc.u-tokyo.ac.jp

expression of SHPS-1 has been shown to be down-regulated in fibroblasts transformed by various oncogene products (*19*). Thus SHPS-1 may be involved in growth factor–induced mitogenesis. In addition, Maile and Clemmons demonstrated that SHPS-1 recruits SHP-2 at the plasma membrane, leading to the dephosphorylation of insulin-like growth factor-I (IGF-I) receptor by SHP-2 in porcine aortic smooth muscle cells (*20*). Timms *et al.* (1999) reported that SHPS-1 acts as a scaffold for the assembly of multiprotein complexs (*21*). These observations suggest a role for SHPS-1 as a signal transducer in various cell types.

The extracellular region of SHPS-1 mediates cell–cell adhesion through the immunoglobulin-like domains. It has been reported that SHPS-1 contributes to macrophage multinucleation (*22*), T-cell activation (*23*), and the tethering of apoptotic cells to phagocytes (*24*) through cell adhesion. Recently, it was shown that SHPS-1 may be involved in the formation of filopodia between neuroblastoma cells (*25*). Thus, SHPS-1 may play a role in the modulation of signal transduction through cell–cell communication. However, its function *in vivo*, especially in skeletal muscle, is not fully understood.

To find genes involved in muscle atrophy or differentiation, we investigated differentially expressed genes in rat extensor digitorum longus (EDL) and soleus muscles after denervation by DNA microarray analysis followed by Northern blot analysis. The results revealed that SHPS-1 is remarkably up-regulated by denervation. In addition, we found that the degree of glycosylation and the localization of SHPS-1 are altered in denervated muscles. SHPS-1 does not interact with SHP-2 in denervated muscles. Taken together, SHPS-1 in skeletal muscle is modulated depending on neural influences, and could play an important role in denervated muscles. This is the first report on the characterization of SHPS-1 in skeletal muscle.

MATERIALS AND METHODS

Animals and Surgical Procedures—Adult male Wistar rats, 8 weeks of age and weighing approximately 250 g, were used in all experiments. Animals were anesthetized with nembutal (50 mg/kg), and the sciatic nerve on the right hindlimb was exposed. To maintain the denervated state for at least 2 weeks, a 1 cm segment of the sciatic nerve was surgically removed. At various time points, rats were deeply anesthetized and killed by decapitation. Extensor digitorum longus (EDL) and soleus muscles from both denervated (right) and innervated (left) legs were immediately removed, frozen in liquid nitrogen, and stored at –80°C

RNA Extraction and Northern Blot Analysis—Total RNA was extracted from frozen EDL and soleus with guanidium thiocyanate as described by Chomczynski and Sacchi (*28*). The total RNA in each sample (10–20 μg) was electrophoresed in a 1.0% agarose gel containing formaldehyde and then transferred to a nylon membrane (Biodyne B, KPL). The membranes were hybridized in hybridization solution (ULTRAhyb, Ambion) according to the manufacturer's instructions with ^{32}P-labeled cDNA fragments encoding mouse SHPS-1 (NCBI Genbank #D87967, 1626–1993), mouse SHP-2 (NCBI Genbank #NM_011202, 1261–1849), human AchRα(NCBI Genbank #NM_000079, 375–887), and human glyceraldehyde-3-phosphate dehydrogenase (GAPDH) (NCBI Genbank #BC023632, 369–717). Autoradiographic signals were analyzed and quantified by a Bioimaging Analyzer System (BAS, Fujifilm).

DNA Microarray Analysis—DNA microarray analysis was performed with Atlas Glass Array Rat 1.0 (CLONTECH) containing 1,090 kinds of gene-specific 80 bp oligonucleotides.

Western Blot Analysis and Deglycosylation—Anti–SHPS-1 rabbit polyclonal antibodies were purchased from Upstate Biotechnology Lake Placid, NY, USA). Anti–SHP-2 mouse monoclonal antibodies were purchased from Transduction Laboratories (Lexington, KY, USA).

Innervated and denervated muscles and brain from rats were homogenized on ice in 2 ml of homogenization buffer [50 mM Tris-HCl (pH 7.5), 1 mM EDTA, 150 mM NaCl, 1% Nonidet P-40 containing 50 mM sodium fluoride, 1 mM phenylmethylsulfonyl fluoride, 1 mM sodium orthovanadate and 0.1% inhibitor mix (WAKO)] with a polytron homogenizer (HITACHI KOUKI). The homogenates were centrifuged at 1,000 × *g* for 2 min at 4°C, and the supernatants were collected. The supernatants were solubilized by rotation for 1 h at 4°C, and centrifuged at 10,000 × *g* for 15 min at 4°C. The resulting supernatants were subjected to immunoblot analysis. Protein concentration was determined using a DC protein assay kit (BIO-RAD). Approximately 20 μg of total homogenates were subjected to 7.5% SDS-PAGE and then transferred to PVDF membranes (finetrap NT-32, Nihon Eido) using a semi-dry electroblotting apparatus. The membranes were blocked for 1 h with 5% non-fat dry milk in phosphate-buffered saline (PBS) containing 0.05% Tween-20 at room temperature. The membranes were incubated with primary antibodies (anti–SHPS-1 at 1:1,000; anti–SHP-2 at 1:5,000) for 30 min at 37°C or overnight at 4°C. The primary antibodies were detected with anti–rabbit IgG horseradish peroxidase–conjugated antibodies (1:5,000) or anti–mouse IgG horseradish peroxidase–conjugated antibodies (1:5,000) for 30 min at 37°C, and then the membranes were incubated in freshly prepared chemiluminescence buffer [100 mM Tris-HCl (pH 8.5), 1.25 mM luminal, 0.2 mM *p*-coumaric acid, 0.009% H_2O_2] for 1 min at room temperature, and exposed to film (hyperfilm™ ECL, Amersham Biosciences).

To examine the glycosylation of SHPS-1, homogenates were boiled in the presence of 1% SDS and 1% 2-mercaptoethanol for 3 min and then subjected to deglycosylation with 2 U/ml of *N*-glycosidase F (Roche) in 50 mM Tris-HCl (pH 7.5) containing 50 mM EDTA, 1% 2-mercaptoethanol, and 1% TritonX-100 for 20 h at 37°C.

Concanavalin A Sepharose Precipitation—Innervated and denervated muscles were homogenized on ice in 2.5 ml of homogenization buffer [50 mM Tris-HCl (pH 7.5), 5 mM EDTA, 5 mM EGTA, 50 mM NaCl, containing 50 mM sodium fluoride, 1 mM phenylmethylsulfonyl fluoride, 1 mM sodium orthovanadate and 0.1% inhibitor mix (WAKO)] with a polytron homogenizer (HITACHI KOUKI). The homogenates were centrifuged at 1,000 × *g* for 2 min at 4°C, and the supernatants were collected. The supernatants were solubilized by rotation for 1 h at 4°C, and centrifuged at 100,000 × *g* for 60 min at 4°C. The

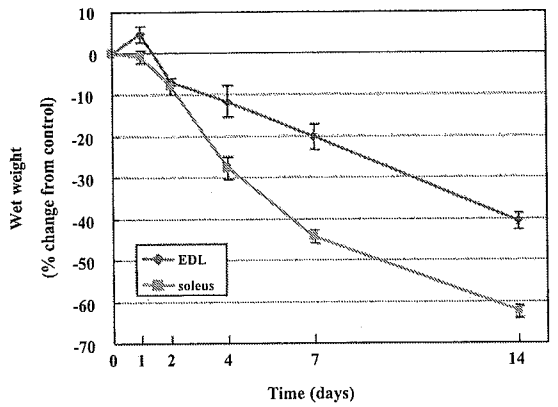

Fig. 1. **Time course of weight loss of rat EDL and soleus muscles after denervation.** Values are means ± SE; $n = 7$.

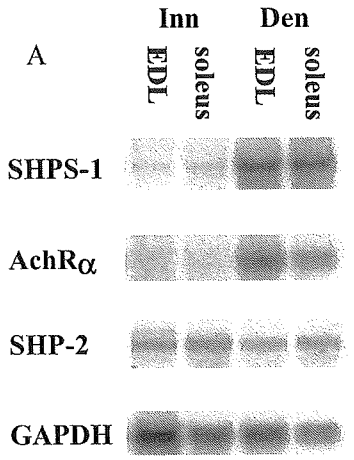

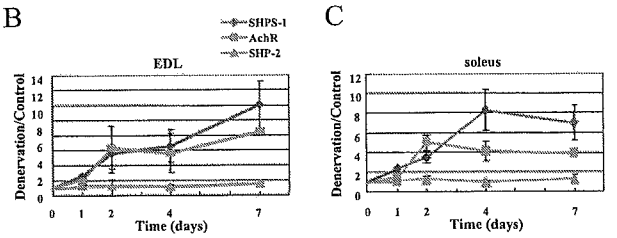

Fig. 2. **Northern blot analysis of SHPS-1, AchRα, and SHP-2.** (A) Bands are the signals of SHPS-1, AchRα and SHP-2 mRNA in innervated (Inn) and 7-day denervated (Den) EDL and soleus muscles. The ratios of mRNA expression of three genes to GAPDH in EDL (B) and soleus (C) muscles 1, 2, 4, and 7 days after denervation are shown. Values are means ± SE; $n = 3$.

resulting supernatants were removed, and the pellets were suspended in 0.8 ml membrane solubilization buffer [20 mM Tris-HCl (pH 7.5), 1% Triton X-100, 150 mM NaCl, 1 mM $MgCl_2$ containing 50 mM sodium fluoride, 1 mM phenylmethylsulfonyl fluoride, 1 mM sodium orthovanadate and 0.1% inhibitor mix (WAKO)]. The suspensions were centrifuged at 100,000 × *g* for 60 min at 4°C, and the resulting supernatants were referred to as the solubilized membrane fractions. The amount of total protein in the solubilized membrane fractions was standardized using a DC protein assay kit (BIO-RAD) before Concanavalin A (ConA) Sepharose precipitation, and the solubilized membrane fractions were incubated with 50 μl ConA Sepharose beads (Amersham Biosciences) overnight at 4°C. The beads were then washed three times with 0.5 ml membrane solubilization buffer, resuspended in SDS sample buffer [50 mM Tris-HCl (pH 6.8), 2% SDS, 6% 2-mercaptoethanol, 1% glycerol (v/v), 0.1% bromophenol blue], and boiled for 3 min at 100°C.

Immunohistochemistry—Tissues were excised, frozen in cold iso-pentane, and sectioned with a cryostat (6 μm). The sections were fixed in 4% paraformaldehyde in PBS for 15 min at 4°C. After pre-incubation with PBS containing 2% bovine serum albumin and 5% heat-inactivated normal goat serum, the sections were incubated with anti–SHPS-1 antibody at 1:250 or anti–SHP-2 antibody, C-18, at 1:250 (Santa Cruz Biotechnology) overnight at 4°C, and then incubated with anti-rabbit IgG antibody–conjugated Oregon green (Molecular Probes) at 1:500 and 2 μg/ml α-bungarotoxin–conjugated rhodamine (Molecular Probes) for 30 min at room temperature. Sections were observed under a fluorescence microscope (OLYMPUS IX70, OLYMPUS).

Statistical Analysis—All values are expressed as mean ± SE. Statistical analysis was performed by Student's *t*-test.

RESULTS

Weight Loss of Rat EDL and Soleus Muscles after Denervation—The decreases in the wet weights of the EDL and soleus muscles with time after denervation are shown in Fig. 1. The wet weights of both muscles were unchanged 1 day after denervation and started to decrease constantly after 2 days. Soleus muscles decreased in wet weight at a faster rate than EDL muscles after 4 days. Finally, soleus muscles decreased to 37.4 ± 1.5% ($n = 7$) of their initial weight and EDL muscles to 59.1 ± 1.9% ($n = 7$) of their initial weight 2 weeks after denervation.

Expression of SHPS-1 mRNA in Denervated Muscles—To identify novel genes involved in the changes in muscles after denervation, we compared mRNA expression in EDL and soleus muscles 7 days after denervation with that in control muscles using DNA microarrays (data not shown). The expressions of several genes were shown to be increased in denervated muscles, and Northern blot analysis was performed for these genes. We found *SHPS-1* to be remarkably up-regulated in both EDL and soleus muscles 7 days after denervation (Fig. 2A). We also found that *AchRα* was dramatically up-regulated after denervation.

To further analyze the expression of these genes, we quantitated the expressions of SHPS-1, SHP-2 and AchRα using mRNA prepared from denervated muscles 1 to 7 days after denervation (Fig. 2, B and C). In EDL muscles, the expressions of SHPS-1 and AchRα increased constantly after denervation, reaching 12-fold (SHPS-1) and 8.5-fold (AchRα) elevations, respectively, after 7 days. The expression of SHP-2, which is known to interact with SHPS-1, did not change after denervation. In

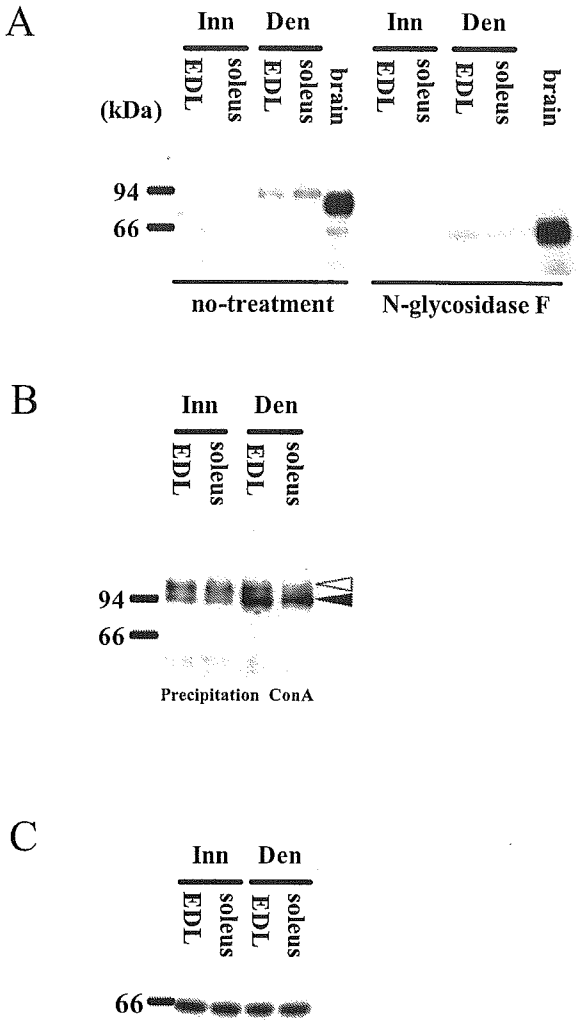

Fig. 3. **Western blot analysis of SHPS-1 and SHP-2 in rat skeletal muscles.** (A) Lysates were prepared from innervated (Inn) and 7-day denervated (Den) muscles, and immunoblotted with anti–SHPS-1 antibody. *N*-glycosidase F treatment was performed as described in "MATERIALS AND METHODS." (B) Solubilized membrane fractions of innervated (Inn) and denervated (Den) muscles were incubated with Con A-Sepharose beads. The proteins bound to Con A-Sepharose were separated by SDS-PAGE and immunoblotted with anti–SHPS-1 antibody. Two major bands were detected, "upper" (open arrowhead) and "lower" (filled arrowhead) SHPS-1. (C) Lysates from innervated (Inn) and 7-day denervated (Den) muscles were immunoblotted with anti–SHP-2 antibody.

soleus muscles, the expression of SHPS-1 increased constantly from 1 to 4 days after denervation, and remained elevated thereafter (a 7-fold increase after 7 days). The expression of AchRα increased rapidly to a 5-fold higher level after 2 days, and then remained high (a 4-fold elevation after 7days). The expression of SHP-2 was also unchanged in soleus muscles.

Glycosylation of SHPS-1 in Innervated and Denervated Muscles—To confirm that the level of the SHPS-1 protein increases in denervated muscles, Western blot analysis was performed with anti–SHPS-1 antibody. As shown in Fig. 3A (left), specific bands with molecular sizes of about 94 kDa were detected in denervated muscles, but not in innervated muscles. In rat brain, the antibody detected a band of about 90 kDa. Because it was thought that these differences in molecular size result from differential glycosylation, we examined shifts in the bands after deglycosylation with *N*-glycosidase F. Deglycosylation converted the molecular sizes of the bands in both denervated muscle and brain samples to about 65 kDa (Fig. 3A, right). Furthermore, we precipitated SHPS-1 with Concanavalin A (Con A) Sepharose. Con A precipitation revealed that a small amount of SHPS-1 protein exists in innervated muscles. Another SHPS-1 species with a molecular mass greater than 94 kDa ("upper" SHPS-1) was detected in both innervated and denervated muscles (Fig. 3B). It was thought that this is the more glycosylated form of SHPS-1. These results indicate that the SHPS-1 protein is expressed in both innervated and denervated muscles and modified in two distinct manners, and that the expression of a form of about 94 kDa ("lower" SHPS-1) increases after denervation, as in the case of the SHPS-1 mRNA. SHP-2 did not undergo any change in denervated muscles (Fig. 3C).

Localization of SHPS-1 in Innervated and Denervated Muscles—To examine whether SHPS-1 is expressed in muscle fibers, we observed EDL and soleus muscle sections immunostained with anti–SHPS-1 antibody. Immunoreactivity was observed as a few small dots in innervated muscles, but diffusely in the plasma membranes of muscle fibers after denervation (Fig. 4). While most fibers were immunoreactive in EDL muscles after denervation (Fig. 4B), only some fibers were immunoreactive in soleus muscles, showing patch-like staining (Fig. 4F). Moreover, anti–SHPS-1 immunoreactivity was also observed at neuromuscular junctions under innervation (Fig. 5A). This localization was confirmed by double-staining with anti–SHPS-1 antibody and rhodamine-conjugated α-bungarotoxin (α-BTX) (Fig. 5C). Since anti–SHPS-1 antibody and α-BTX stainings colocalized in denervated muscles, it was confirmed that anti–SHPS-1 immunoreactivity, like AchRs, localizes on plasma membranes in muscle fibers (Fig. 5, B and D).

We also stained muscle sections with anti–SHP-2 antibody. Immunoreactivity was observed in the cytoplasm in both innervated and denervated muscles (Fig. 6). SHP-2 was not localized at neuromuscular junctions. These observations imply that SHP-2 is not regulated by innervation.

DISCUSSION

Previously, we found by DNA microarray analysis that another gene, ARPP16/19, is highly up-regulated in denervated rat muscle (27). However, this protein is a cytoplasmic adaptor and no physiological role was implicated. In this report, we provide the first demonstration that SHPS-1 is highly expressed in rat denervated skeletal muscles. We also show that the expression, glycosylation, and localization of SHPS-1 are altered after denervation. In contrast, SHP-2 does not change its expression or localization after denervation. These results suggest that SHP-2 is not involved in SHPS-1 function in denervated muscles. Taken together, SHPS-1 and SHP-2 may be regulated in different pathways in rat skeletal muscles.

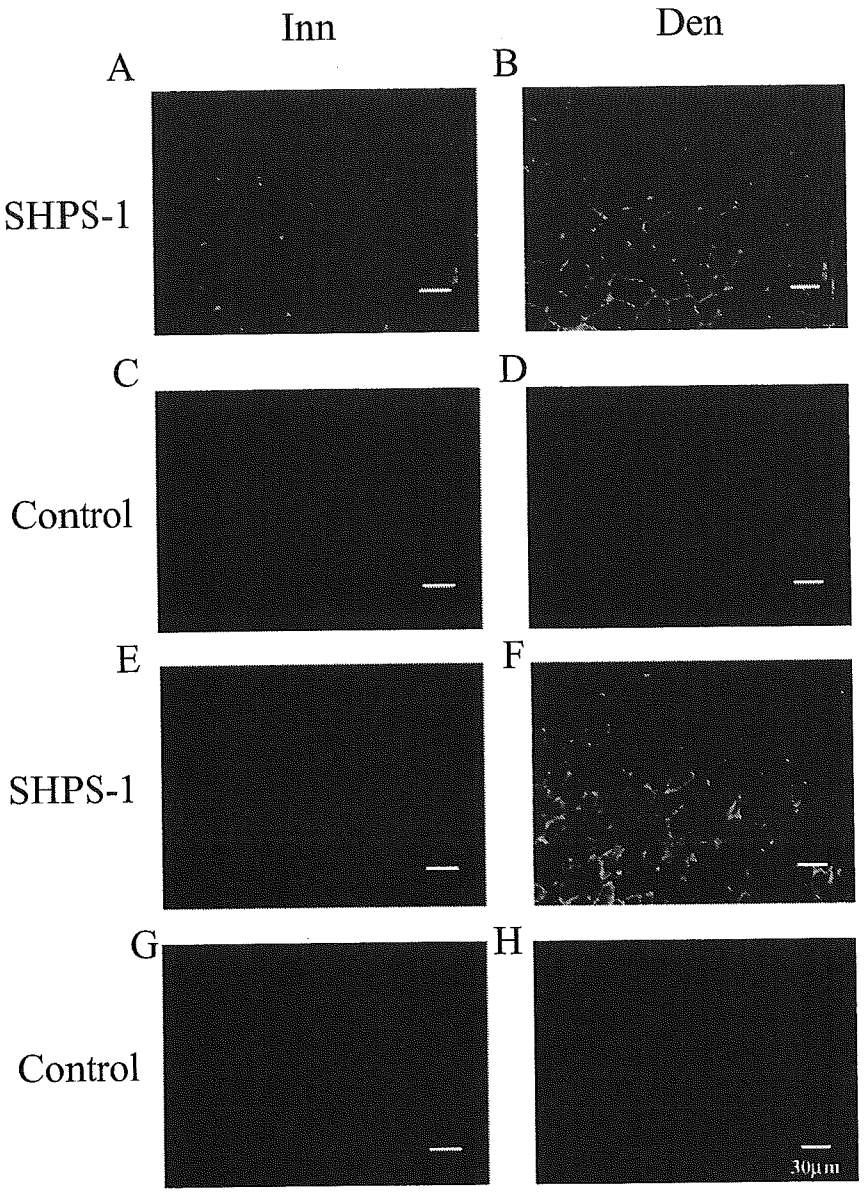

Fig. 4. **Localization of SHPS-1 in rat skeletal muscles.** Cross-sections of innervated (A, E) and 7-day denervated (B, F) muscles stained with anti–SHPS-1 antibody. A series of sections was stained without a primary antibody as a control (C, D, G, H). (A–D) EDL, (E–H) soleus ; Bar = 30 μm

We have demonstrated that the expression of SHPS-1, although very low in innervated muscles, increases in denervated muscle in a manner similar to that of AchRα. AchR is one of the most important cation channels for neuromuscular transmission. It is concentrated at NMJs, and is remarkably up-regulated after denervation (*28*). It is thought that this is a compensation mechanism for a loss of acetylcholine. Often, other proteins induced by denervation are up-regulated at far lower rates than the AchRα, but the SHPS-1 mRNA increases remarkably (Fig. 2). This implies that the increase in the expression of SHPS-1 may compensate for a loss of neural stimuli, and that SHPS-1 may play a role in innervation.

The levels of SHPS-1 and AChRαmRNA are relatively low under innervation and rise rapidly following denervation. In addition, we have observed that SHPS-1 immunoreactivity localizes at NMJs in innervated muscles and throughout the plasma membrane in denervated muscles. Although AchR and its interacting proteins, MuSK and rapsyn, are expressed at low levels and are restricted to NMJs under innervation, denervation induces increases in their expressions, and their localization becomes extrasynaptic (*29–31*). NCAM and BEN/SC1/DM-GRASP, members of the immunoglobulin superfamily, also show these alterations (*32–36*). NCAM is thought to play an important role in neurogenesis through cell–cell contacts (*37, 38*). In recent studies, it was reported that SHPS-1 binds to CD47 via its extracellular domain, and this interaction is implicated in synapse formation or maintenance (*39*). Taken together, it is possible that SHPS-1 is involved in nerve–muscle cell interaction.

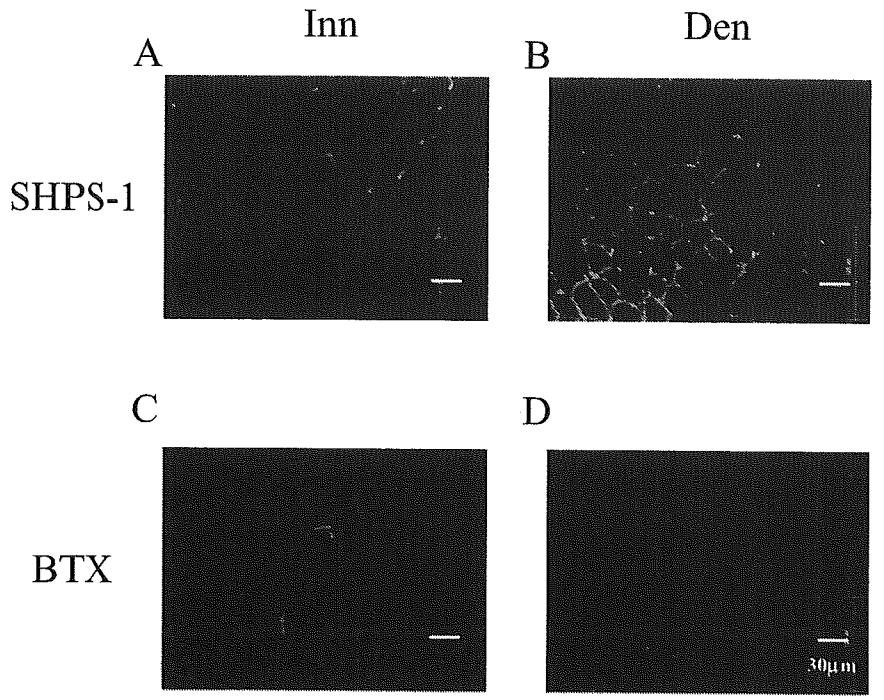

Fig. 5. **Co-localization of SHPS-1 and AchR in innervated and denervated muscles.** Cross-sections of innervated and 7-day denervated EDL muscle were double-stained with anti–SHPS-1 antibody (A, B) and rhodamine-conjugated α-bungarotoxin (BTX) (C, D). (A, C) innervated (B, D) denervated; Bar = 30 μm.

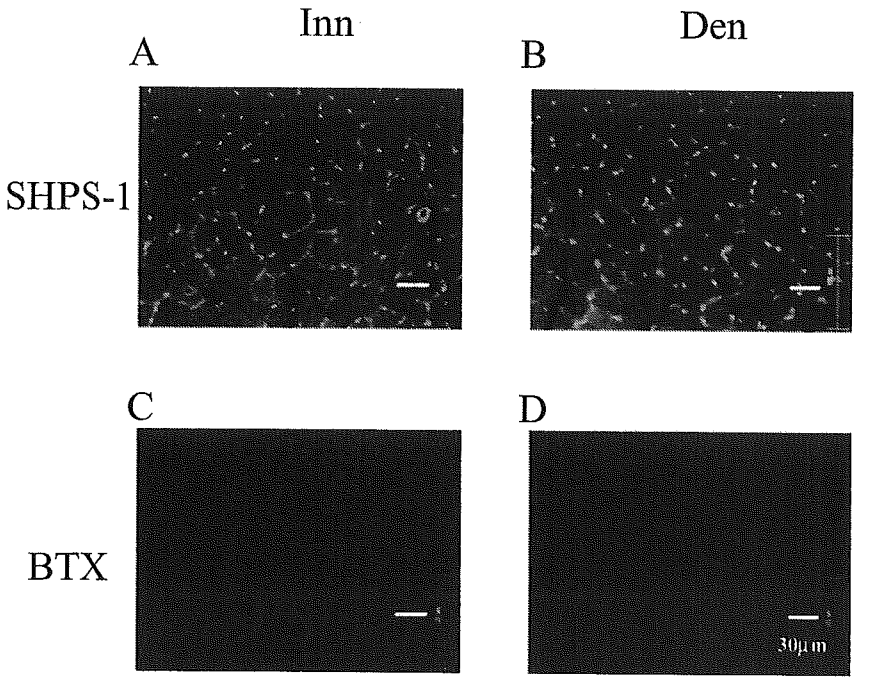

Fig. 6. **Immunohistochemistry of SHP-2 in EDL muscle.** Cross-sections of innervated and 7-day denervated EDL muscle were stained with anti–SHP-2 antibody (A, B). A series of sections was stained without a primary antibody as a control (C, D). (A, C)innervated (B, D)denervated ; Bar = 30 μm.

The rates of increase of SHPS-1 expression and immunoreactivity with the anti–SHPS-1 antibody differ slightly between EDL and soleus muscles. These differences may be due to the difference in fiber types. Muscle atrophy progresses at different rates in EDL and soleus muscles. Thus, differences in the nature of the muscle fibers might account for the small difference in SHPS-1 expression.

The glycosylation of SHPS-1 is regulated in tissue-specific manner, and the isoform in skeletal muscle is different from that in brain. Moreover, two distinct isoforms with different affinities for Con A exist in skeletal muscle, and the expression of only one form increases after denervation. Generally, glycosylation modulates the adhesion activity of glycoproteins, and it is reported that the aberrant *N*-glycosylation of SHPS-1 impairs its abil-

ity to bind CD47 (*40*). It is possible that SHPS-1 functions with different activities in innervated muscles and denervated muscles.

SHP-2 has been reported to interact with the tyrosine-phosphorylated cytoplasmic domain of SHPS-1 (*9*, *10*), and to regulate EGF, insulin, and the IGF-I signaling pathway (*10*, *20*). In our experiments, since the expression and localization of SHP-2 did not change after denervation, SHP-2 appears to be independent of the intracellular changes caused by denervation. We also demonstrated that SHP-2 does not concentrate at NMJs. Tanowitz *et al.* reported that SHP-2 is concentrated at NMJs in mouse diaphragm (*41*). But Mei *et al.* showed that SHP-2 localizes in the cytoplasm of muscle fibers in rat hindlimbs (*42*). We also examined SHP-2 in rat hindlimb muscles and our results are consistent with the latter results. Additionally, we performed co-immunoprecipitation experiments but could not detect any interaction between SHPS-1 and SHP-2 in either innervated or denervated muscles (data not shown). Our results suggest that SHPS-1 interacts with novel proteins other than SHP-2, and regulates intracellular signaling in response to changes caused by denervation in skeletal muscle.

Little is known about SHPS-1 except for its interactions with SHP-1 and SHP-2, and its participation in cell adhesion. Most previous studies utilized cultured cells; therefore, how SHPS-1 functions *in vivo* has remained unclear, even in brain where it is highly expressed. Our results contribute new information about the function of SHPS-1 *in vivo*, and suggest that SHPS-1 plays an important role in denervated and undifferentiated skeletal muscle.

This work was supported in part by a Grant from the Ministry of Health, Welfare and Labor, Japan.

REFERENCES

1. Adams, L., Carlson, B.M., Henderson, L., and Goldman, D. (1995) Adaptation of nicotinic acetylcholine receptor, myogenin, and MRF4 gene expression to long-term muscle denervation. *J. Cell Biol.* **131**, 1341–1349
2. Eftimie, R., Brenner, H.R., and Buonanno, A. (1991) Myogenin and MyoD join a family of skeletal muscle genes regulated by electrical activity. *Proc. Natl Acad. Sci. USA* **98**, 14440–14445
3. Weis, J. (1994) Jun, Fos, MyoD1, and myogenin proteins are increased in skeletal muscle fiber nuclei after denervation. *Acta Neuropathol. (Berl)* **87**, 63–70
4. Weis, J., Kaussen, M., Calvo, S., and Buonanno, A. (2000) Denervation induces a rapid nuclear accumulation of MRF4 in mature myofibers. *Dev. Dyn.* **218**, 438–451
5. Witzemann, V. and Sakmann, B. (1991) Differential regulation of MyoD and myogenin mRNA levels by nerve induced muscle activity. *FEBS Lett.* **282**, 259–264
6. Huey, K.A. and Bodine, S.C. (1998) Changes in myosin mRNA and protein expression in denervated rat soleus and tibialis anterior. *Eur. J. Biochem.* **256**, 45–50
7. Robin, N.M., David, J.P., and Shannon, E.D. (1996) Regulation of myosin heavy chain expression in adult rat hindlimb muscles during short-term paralysis : comparison of denervation and tetrodotoxin-induced neural inactivation. *FEBS Lett.* **391**, 39–44
8. Witzemann, V., Brenner, H.R., and Sakmann, B. (1991) Neural factors regulate AchR subunit mRNAs at rat neuromuscular synapses. *J. Cell Biol.* **114**, 125–141
9. Fujioka, Y., Matozaki, T., Noguchi, T., Iwamatsu, A., Yamao, T., Takahashi, N., Tsuda, M., Takada, T., Kasuga, M. (1996) A novel membrane glycoprotein, SHPS-1, that binds the SH2-domain-containing protein tyrosine phosphatase SHP-2 in response to mitogens and cell adhesion. *Mol. Cell. Biol.* **16**, 6887–6899
10. Kharitonenkov, A., Chen, Z., Sures, I., Wang, H., Schilling, J., and Ullrich, A. (1997) A family of proteins that inhibit signaling through tyrosine kinase receptors. *Nature* **386**, 181–186
11. Ohnishi, H., Kubota, M., Ohtake, A., Sato, K., and Sano, S. (1996) Activation of protein-tyrosine phosphatase SH-PTP2 by a tyrosine-based activation motif of a novel brain molecule. *J. Biol. Chem.* **271**, 25569–25574
12. Saginario, C., Sterling, H., Beckers, C., Kobayahi, R., Solimena, M., Ullu, E., and Vignery, A. (1998) MFR, a putative receptor mediating the fusion of macrophases. *Mol. Cell. Biol.* **18**, 6213–6223
13. Comu, S., Weng, W., Olinsky, S., Ishwad, P., Mi, Z., Hempel, J., Watkins, S., Lagenaur, C.F., and Narayanan, V. (1997) The murine P84 neural adhesion molecule is SHPS-1, a member of the phosphatase-binding protein family. *J. Neurosci.* **17**, 8702–8710
14. Veillette, A., Thibaudeau, E., and Latour, S. (1998) High expression of inhibitory receptor SHPS-1 and its association with protein-tyrosine phosphatase SHP-1 in macrophages. *J. Biol. Chem.* **273**, 22719–22728
15. Seiffert, M., Cant, C., Chen, Z., Rappold, I., Brugger, W., Kanz, L., Brown, E.J., Ullrich, A., and Bühring, H.J. (1999) Human signal-regulatory protein is expressed on normal, but not on subsets of leukemic myeloid cells and mediates cellular adhesion involving its counterreceptor CD47. *Blood* **94**, 3633–3643
16. Sano, S., Ohnishi, H., and Kubota, M. (1999) Gene structure of mouse BIT/SHPS-1. *Biochem. J.* **344**, 667–675
17. Takada, T., Matozaki, T., Takeda, H., Fukunaga, K., Noguchi, T., Fujioka, Y., Okazaki, I., Tsuda, M., Yamao, T., Ochi, F., and Kasuga, M. (1998) Roles of the complex formation of SHPS-1 with SHP-2 in insulin-stimulated mitogen-activated protein kinase activation. *J. Biol. Chem.* **273**, 9234–9242
18. Kharitonenkov, A., Chen, Z., Sures, I., Wang, H., Schilling, J., and Ullrich, A. (1997) A family of proteins that inhibit signaling through tyrosine kinase receptors. *Nature* **386**, 181–186
19. Machida, K., Matsuda, S., Yamaki, K., Senga, T., Thant, A.A., Kurata, H., Miyazaki, K., Hayashi, K., Okuda, T., Kitamura, T., Hayakawa, T., and Hamaguchi M. (2000) v-Src suppresses SHPS-1 expression via the Ras-MAP kinase pathway to promote the oncogenic growth of cells. *Oncogene* **19**, 1710–1718
20. Maile, L.A. and Clemmons, D.R. (2002) Regulation of insulin-like growth factor I receptor dephosphorylation by SHPS-1 and the tyrosine phosphatase SHP-2. *J. Biol. Chem.* **277**, 8955–8960
21. Timms, J.F., Swanson, K.D., Marie-Cardine, A., Raab, M., Rudd, C.E., Schraven, B., and Neel, B.G. (1999) SHPS-1 is a scaffold for assembling distinct adhesion-regulated multi-protein complexes in macrophages. *Curr. Biol.* **9**, 927–930
22. Han, X., Sterling, H., Chen, Y., Saginario. C., Brown, E.J., Frazier, W.A., Lindberg, F.P., and Vignery, A. (2000) CD47, a ligand for the macrophage fusion receptor, participates in macrophage multinucleation. *J. Biol. Chem.* **275**, 37984–37992
23. Seiffert, M., Brossart, P., Cant, C., Cella, M., Colonna, M., Brugger, W., Kanz, L., Ullrich, A., and Bühring, H.-J. (2001) Signal-regulatory protein α (SIRPα) but not SIRPβ is involved in T-cell activation, binds to CD47 with high affinity, and is expressed on immature $CD34^+$ $CD38^-$ hematopoietic cells. *Blood* **97**, 2741–2749
24. Tada, K., Tanaka, M., Hanayama, R., Miwa, K., Shinohara, A., Iwamatsu, A., Nagata, S. (2003) Tethering of apoptotic cells to phagocytes through binding of CD47 to Src homology 2 domain-bearing protein tyrosine phosphatase substrate-1. *J. Immunol.* **171**, 5718–5726
25. Miyashita, M., Ohnishi, H., Okazawa, H., Tomonaga, H., Hayashi, A., Fujimoto, T.-T., Furuya, N., and Matozaki, T. (2004) Promotion of neurite and filopodium formation by

CD47: roles of integrins, Rac, and Cdc42. *Mol. Biol. Cell* **15**, 3950–3963
26. Chomczynski, P. and Sacchi, N. (1987) Single-step method of RNA isolation by acid guanidium thiocyanate-phenol-chloroform extraction. *Anal. Biochem.* **162**, 156–159
27. Yoshikawa, A., Mitsuhashi, H., Sasagawa, N., Tsukahara, T., Hayashi, Y., Nishino, I., Goto, Y., and Ishiura, S. (2003) Expression of ARPP-16/19 in rat denervated skeletal muscle. *J. Biochem.* **134**, 57–61
28. Tsay, H.-J. and Schmidt, J. (1989) Skeletal muscle denervation activates acetylcholine receptor genes. *J. Cell Biol.* **108**, 1523–1526
29. Baldwin, T.J., Theriot, J.A., Yoshihara, C.M., and Burden, S.J. (1998) Regulation of transcript encoding the 43K subsynaptic protein during development and after denervation. *Development* **104**, 557–564
30. Valenzuela, D.M., Stitt, T.N., DiStefano, P.S., Rojas, E., Mattsson, K., Compton, D.L., Nunez, L., Park, J.S., Stark, J.L., Gies, D.R., Thomas, S., LeBeau, M.M., Fernald, A.A., Copeland, N.G., Jenkins, N.A., Burden, S.J., Glass, D.J., and Yancopoulos, G.D. (1995) Receptor tyrosine kinase specific for the skeletal muscle lineage: expression in embryonic muscle, at the neuromuscular junction, and after injury. *Neuron* **15**, 573–584
31. Bowen, D.C., Park, J.S., Bodine, S., Stark, J.L., Valenzuela, D.M., Stitt, T.N., Yancopoulos, G.D., Lindsay, R.M., Glass, D.J., and DiStefano, P.S. (1998) Localization and regulation of MuSK at the neuromuscular junction. *Dev. Biol.* **199**, 309–319
32. Rieger, F., Grumet, M., and Edelman, G.M. (1985) N-CAM at the vertebrate neuromuscular junction. *J. Cell Biol.* **101**, 285–293
33. Covault, J., Merlie, J.P., Goridis, C., and Sanes, J.R. (1986) Molecular forms of N-CAM and its RNA in developing and denervated skeletal muscle. *J. Cell Biol.* **102**, 731–739
34. Covault, J. and Sanes J.R. (1985) Neural cell adhesion molecule (N-CAM) accumulates in denervated and paralyzed skeletal muscles. *Proc. Natl Acad. Sci. USA* **82**, 4544–4548
35. Daniloff, J.K., Levi, G., Grumet, M., Rieger, F., and Edelman, G.M. (1986) Altered expression of neural cell adhesion molecules induced by nerve injury and repair. *J. Cell Biol.* **103**, 929–945
36. Fournier-Thibault, C., Pourquié, O., Rouaud, T., and Le Douarin, N.M. (1999) BEN/SC1/DM-GRASP expression during neuromuscular development: a cell adhesion molecule regulated by innervation. *J. Neurosci.* **19**, 1382–1392
37. Seki, T. and Rutishauser, U. (1998) Removal of polysialic acid-neural cell adhesion molecule induces aberrant mossy fiber innervation and ectopic synaptogenesis in the hippocampus. *J. Neurosci.* **18**, 3757–3766
38. Rafuse, V.F., Polo-Parada, L., and Landmesser, L.T. (2000) Structural and functional alterations of neuromuscular junctions in NCAM-deficient mice. *J. Neurosci.* **20**, 6529–6539
39. Mi, Z.P., Jiang, P., Weng, W.L., Lindberg, F.P., Narayanan, V., and Lagenaur, C.F. (2000) Expression of a synapse-associated membrane protein, p84/SHPS-1, and its ligand, IAP/CD47, in mouse retina. *J. Comp. Neurol.* **416**, 335–344
40. Ogura, T., Noguchi, T., Murai-Takebe, R., Hosooka, T., Honma, N., and Kasuga, M. (2004) Resistance of B16 melanoma cells to CD47-induced negative regulation of motility as a result of aberrant *N*-glycosylation of SHPS-1. *J. Biol. Chem.* **279**, 13711–13720
41. Tanowitz, M., Si, J., Yu, D.-H., Feng, G.-S., and Mei, L. (1999) Regulation of neuregulin-mediated acetylcholine receptor synthesis by protein tyrosine phosphatase SHP-2. *J. Neurosci.* **19**, 9426–9435
42. Mei, L., Kachinsky, A.M., Seiden, J.E., Kuncl, R.W., Miller, J.B., and Huganir R.L. (1996) Differential expression of PTP1D, a protein tyrosine phosphatase with two SH2 domains, in slow and fast skeletal muscle fibers. *Exp. Cell Res.* **224**, 379–390

TOPICS トピックス

筋強直性ジストロフィーの分子生物学的発症機構

KEYWORDS
筋強直性ジストロフィー，トリプレット・リピート病，RNA gain of function

1. はじめに

1992年に筋強直性ジストロフィー(Myotonic Dystrophy；DM)の責任遺伝子が同定されたとの発表は，世界に多くの衝撃をもたらした．DMは脆弱X症候群やハンチントン病などとともに，世界で初めて発見されたトリプレット・リピート病のひとつであり，患者ではCTGトリプレット・リピートの伸長が見られる．DMは優性の形式で発症する遺伝病だが，その遺伝子変異が通常では考えられない非翻訳領域に存在していたのである．DM研究は初期の混迷した時期を経て2000年あたりから急速な進展を見せ，最近ようやく発症機構解明の手がかりが得られようとしている．本稿では最近のDM研究の成果を分子生物学的な立場から解説する．

2. DMのサブタイプ

1992年に初めて見つかったDMの遺伝子変異は，第19番染色体におけるCTGトリプレット・リピートの伸長であった[1~3]．一方でCTGトリプレット・リピートの伸長が見られないDM患者の存在も知られていたが，2001年には第3番染色体のCCTGクアドラプレット・リピートの伸長が原因で起こるDMの存在が報告された[4]．それ以降，CTGトリプレット・リピートの伸長が原因のDMをDM1，CCTGクアドラプレット・リピートの伸長が原因のDMをDM2と呼ぶようになった．以降，本稿でもその表記に従う．

3. DMの責任遺伝子

DM1の責任遺伝子として同定されたDM protein kinase(DMPK)の遺伝子構造を図1に示す．この遺伝子産物はセリン・スレオニンリン酸化酵素である．線虫やショウジョウバエ，マウス，ラットなどでヒトDMPKと相同性を示す分子が見つかっており，これらはmyotonic dystrophy family of protein kinases(MDFPK)と呼ばれている．ヒトの場合，停止コドンを過ぎた後の3′側非翻訳領域にCTGトリプレット・リピートがあり，正常対照でも5~30回の繰返しをもつのに対し，DM患者では100回以上，多いものでは数千もの繰返しをもつことが判明している．通常の優性遺伝病なら，悪性蛋白質の発現という機能獲得型の遺伝子変異が一般的であるが，DM1の遺伝子変異はアミノ酸をコードしない領域にあるため，DM患者で悪性機能をもったDMPKが発現するようなことはない．

ここにDM2の責任遺伝子であるZNF9の遺伝子構造も図1に示した．ZNF9はCellular Nucleic acid-Binding Protein(CNBP)とも呼ばれるジンクフィンガー蛋白質であり，DNAと結合する転写因子として発生調節に関与することが示唆されている．このZNF9の第一イントロンにCCTGリピートが存在し，正常対照では百数十なのに対して，DM2患者では平均して5,000にまで伸長していることが報告されている．DM2の場合も，発現蛋白質に異常が入る変異ではない．

4. DMのモデルマウス

DM研究の最大の転換点は1996年に報告されたDMPKノックアウトマウス，トランスジェニックマウスであった[5,6]．先に述べたようにDMでは患者においても正常型のDMPKが発現すると考えられるため，以前はCTGリピートの伸長によりDMPK自身の発現量に変化が生じ，それがDM発症につながっていくという仮説がDM研究において有力な時期があった．ヒトにおけるDMの症状は，筋緊張，筋萎縮を主症状とし，白内障，精神遅滞，性腺萎縮，耐糖能障害，前頭部脱毛などの全身に渡る症状を併発するのが特徴であり，DMPKノックアウトマウス，トランスジ

0485-1420/05/¥250/論文/JCLS

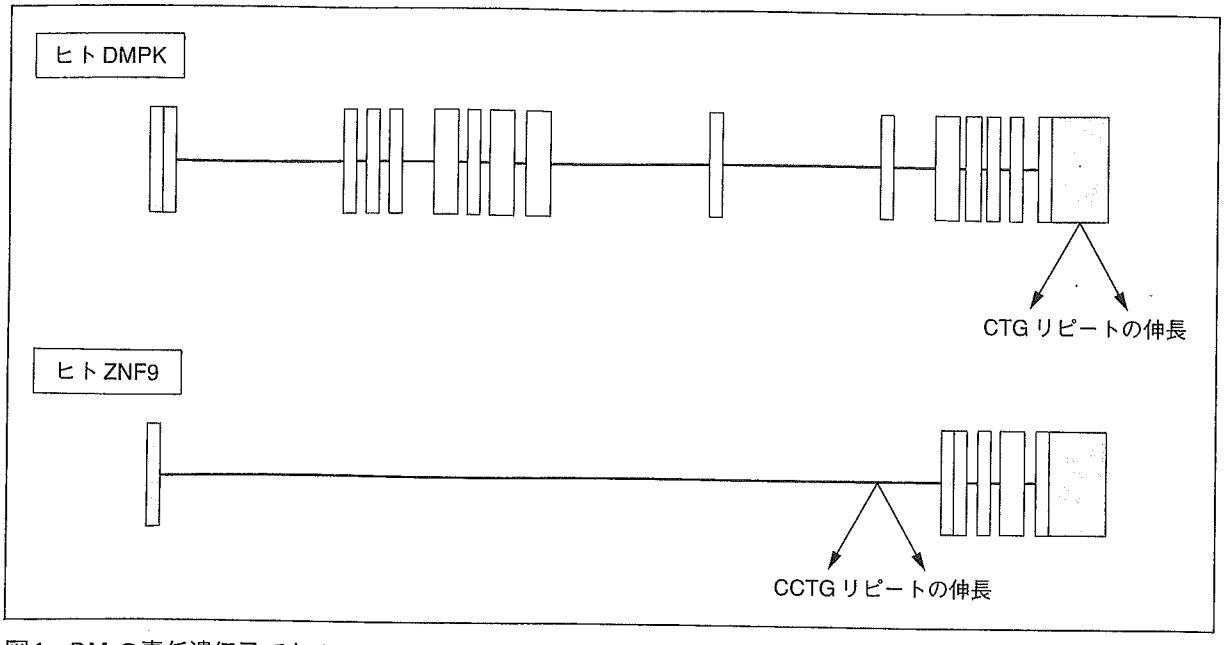

図1　DMの責任遺伝子であるDMPKとZNF9の模式図
灰色のボックスは非翻訳領域を表し，白いボックスはアミノ酸コード領域を表す．黒線はイントロン領域である．イントロンを含めたDMPKのサイズは約12 kbpであり，同様にZNF9は約14 kbpである．DMPK，ZNF9ともに，アミノ酸をコードしない領域にリピート伸長という遺伝子変異が見られる．

ェニックマウスでも，これらの症状が再現されることが期待された．しかし結果はこのようなヒトDMの多様な表現型を再現したとは言い難く，このことから，DM発症におけるDMPK発現量の量的効果説は一気に下火となってしまった．2004年にDMPKトランスジェニックマウスに筋障害が現れたとする報告などもあるが[7]，現在ではDMPKの発現量変化だけではDMの症状を説明できないとの見方が一般的である．

一方で，CTGリピートのみを過剰発現させたマウス[8~10]，CUG binding protein(CUGBP)トランスジェニックマウス[11,12]，Muscleblind-like(MBNL)ノックアウトマウス[13]などでヒトDMの症状を示唆する結果がこれまでに得られている．このCUGBP，MBNLという分子は，伸長したリピートRNAの生理機能追究の過程で発見されてきたRNA結合蛋白質である．次項でこれらRNA結合蛋白質がかかわるDM発症機構の仮説について説明する．

5. リピートRNAに対するRNA結合蛋白質の異常結合

DM1で見られるCTGリピート，DM2で見られるCCTGリピートはともにゲノムから転写されてCUG，CCUGリピートとなる．これらのリピートは一本鎖RNAの状態では自身でヘアピンのような異常な立体構造を形成する．一方で細胞内には多くのRNA結合蛋白質が存在しており，そのなかにCUG，CCUGヘアピン構造を認識し，結合するものがあることが報告された．そのRNA結合蛋白質がCUGBP，MBNLと呼ばれるものである．CUGBP，MBNLは別々に発見されたものであるが，これらCUGBP，MBNLの発見により，患者だけで見られる異常な立体構造をとったリピートRNAとRNA結合蛋白質の結合という事象が，DM患者だけで起こりうる第一義の現象であるという考えが現在では一般的になってきた．遺伝子変異がRNAレベルでの新たな機能獲得につながる例であり，RNA gain of functionと呼ばれるようになった．

われわれは，酵母系を用いてリピートRNAとCUGBPやMBNLとのRNA-蛋白質結合能を計測することを試みた[14,15]．CUGBPはCUGリピートとわずかながら結合するようだが，それよりもUGUGUG…といったUG二塩基リピートと良

綜　説

筋強直性ジストロフィー発症のメカニズム

石浦章一

Molecular pathways to myotonic dystrophy

Shoichi Ishiura
Department of Life Sciences, Graduate School of Arts and Sciences,
The University of Tokyo

Abstract

Myotonic dystrophy (DM), the most common form of adult-onset muscular dystrophy, comprises at least 2 sub-types, DM1 and DM2. DM1 is caused by the expansion of a CTG repeat located in the 3′ untranslated region (3UTR) of the DM protein kinase (*DMPK*) gene. Recently, the expansion of a CCTG tetranucleotide repeat located in the first intron of the *ZNF9* gene was identified as the mutation responsible for DM2. Since both DM1 and DM2 are caused by the expansion of repetitive sequences, some common factors that interact with these sequences might be involved in the pathogenesis of DM. MBNL (muscleblind) 1 is a candidate for such factors and is thought to be sequestered by the expanded forms of DM transcripts.

Key words: myotonic dystrophy, triplet repeat, DMPK, ZNF9, MBNL1

はじめに

筋強直性ジストロフィーは全身性の優性遺伝疾患で，筋強直のみならず，心臓の伝導障害，インスリン耐性，白内障，内分泌異常，性腺萎縮，睡眠障害など多くの症状が現れる[1,2]．その原因は，第19染色体長腕にある*DMPK* (dystrophia myotonica protein kinase) 遺伝子の3′非翻訳領域にあるCTGトリプレットの増加であることが，1992年に明らかにされた．このDM1 (dystrophia myotonica 1) 家系では，母親から遺伝子を受け継いだときに大幅にリピート数が増加することが多いことが明らかになり，発症が早くなり症状も重いという‘表現促進現象’が認められた．

1990年代になって，DM1とは異なる座位に変異が起こって，ミオトニアをはじめ，よく似た全身症状を呈する家系が見つかり，proximal myotonic myopathy (PROMM) と名付けられた．この遺伝子は第3染色体に存在することがわかり，DM2と名付けられた[3]．DM1との大きな違いは，DM1では精神遅滞などの発達障害を呈する先天型が存在するのに対し，DM2ではそのようなものは認められないという点である．

1. DM1

図1に第19染色体*DMPK*遺伝子座近くの構造を示す．*DMPK*遺伝子は15個のエキソン

東京大学大学院総合文化研究科

0047-1852/05/¥50/頁/JCLS

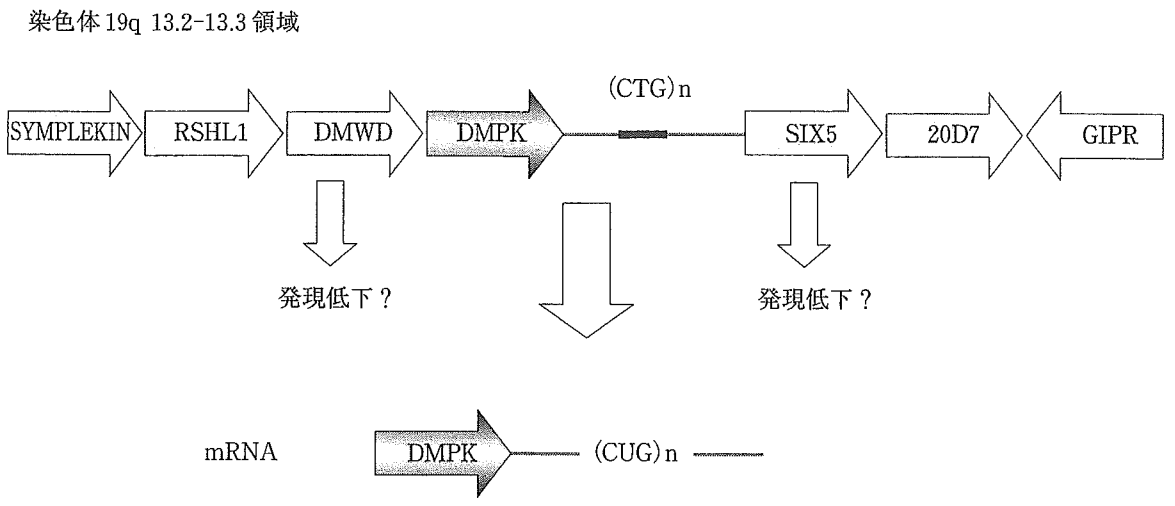

図1 DMPK座付近の遺伝子

*DMPK*遺伝子の上流にはDMWD，下流には*SIX5*遺伝子が存在するが，リピートはDMPKのmRNAにしか転写されない．

からできており，第15エキソンには終止コドンとCTGトリプレットリピートが存在する[4]．*DMPK*遺伝子の下流にはホメオドメイン蛋白質SIX5をコードする遺伝子が，上流には精巣発現遺伝子*DMWD*がある．

CTGの長さは，患者では200リピートを超え，4,000リピートにもなる例が報告されている．また，50-200リピートまでをpremutationと呼び，伸長の一段階前と考えられている．DM1にも，通常のトリプレットリピート病にみられるような表現促進現象(anticipation: 親よりも子，子よりも孫，の方が症状も重く発症時期も早い．発症時期とリピート数には反比例の関係がある)が認められる．このとき，奇妙なことに母親からリピートが伝わったときに伸びやすい，という事実が報告されている．またDM1の患者は，一般にリピートが伸長したアリールと通常の長さのアリールを1本ずつもっている．これらからは等量のmRNAが作られていることがわかっている．

DM1は優性遺伝する病気である．ところが変異が3′非翻訳領域に存在するため，作られる蛋白質は質的に同じである．同じものができるのになぜ病気は優性遺伝するのか，という点についてはいくつもの仮説が提出されていた．

2. ハプロ不全説

最初に提出されたのは，DMPK蛋白質の量が足りなくなる，というハプロ不全説であった．これは，非翻訳領域にあるリピートの伸長のおかげで翻訳効率が悪くなり，DMPK蛋白質の合成が滞るのではないかというものであった．著者らも人工的に発現させたリピート長の異なるDMPK cDNAを用いた実験で，リピートが160になるとリピート5に比べて確かに翻訳されたDMPKの量が少なくなることを示し，リピートが長くなると翻訳効率が落ちることを証明した[5]．

ところが，DMPKノックアウトマウスを作ってみると，ヒトDMでみられるような全身性の症状はみられず，せいぜい心臓の伝導障害があるかどうか，ということがわかり，DMPKが足りないだけではDMでみられるような症状が説明できない，ということになってきた．また，*DMPK*遺伝子の点突然変異でDMが引き起こされる例が見当たらず，DMPKの量の低下(活性低下)では説明がつかない，というのが定説になっている．

3. 近隣遺伝子発現制御説

次に提出されたのが，近隣遺伝子ハプロ不全

説である．**図1**で明らかなように，伸長したリピートは下流にある*SIX5*遺伝子のプロモーターの近傍に存在する．この遺伝子は，ショウジョウバエの目の発生に関与する転写因子*sine oculis*遺伝子に似ていて，マウスでノックアウトすると白内障を呈する．すなわち，*DMPK*にあるCTGリピートが*SIX5*の転写量を負に調節しているのではないか，というものである(注：このリピートはDMPKのmRNAに転写されCUGリピートになるが，mRNAレベルではSIX5には無関係となる)．しかしながらDMに関係していてもせいぜい白内障だけであり，現在ではあまり注目されていない．

同様に*DMPK*のすぐ上流にある*DMWD*遺伝子は精巣に発現しており，DMの男性不妊に関係するのではないかと疑われている．しかし，これについての証拠はあまりない．また，DMに特徴的なIgGの低下に関係すると疑われているIgG受容体遺伝子*FCGRT*は，このDMPK座から少し離れていて，この関与も定かではない．

4. 長いリピートをもつmRNAが犯人？

患者細胞を使って，*in situ* hybridizationの実験を行ってみると，長いリピートをもつmRNAが核に局在していることが明らかになってきた．続いて，CTGリピートだけでも症状が出てくるらしいことがわかってきた．

Mankodiらは，骨格筋アクチン遺伝子のプロモーターの下流に伸長したCTGを入れただけのコンストラクトをマウスに発現させたところ，ミオトニアなどDM1の筋肉症状を再現したのである[6]．残念ながらこのマウスではCTGは筋肉にしか発現しないため，全身症状をみるまでには至らなかったが，DMPKの方ではなく，CTGリピートが何らかの機構を介して症状を発現させていることは間違いない，と信じられるようになった．また，挿入したCTGリピートはゲノムのどこに挿入されたかもわからないのに，DMと同じ症状になったということは，近隣遺伝子説にとってダメージは大きかった．

5. DM2の発見

2001年に，DM2が第3染色体の*ZNF9*(zinc finger protein 9)遺伝子の第1イントロンにあるCCTGリピートの伸長で起こることが発見され，大きな反響を呼んだ(**図2**)．ZNF9には，7つのC2H2型ジンクフィンガーモチーフがあり，DNAおよびRNAに結合することができる．ZNFはβミオシン重鎖やコロニー刺激因子1の転写調節にかかわるといわれている．ところが，リン酸化酵素DMPKと転写因子ZNF9の間には何も機能についての共通性がなく，しかもリピートも片方は三塩基，片方は四塩基であった．両方とも，翻訳されるところにリピートがなかった．

DM2のリピート長は，患者では75–11,000にも及んだが，DM1のようなリピート長と発症時期の間の逆相関はみられていない．*ZNF9*のイントロンには，$(TG)_n(TCTG)_n(CCTG)_n$という繰り返しがあり，正常ではこの最後の$(CCTG)_n$のところに中断が入っている．

しかし，このCCTGリピートは，プレmRNAに入っていてもスプライスされてしまい，成熟mRNAの中には認められない．ということは，病気がもし三または四塩基リピートに原因があるとすると，mRNAに転写されたあと，しかも蛋白質に翻訳される前に，何らかの異常が生じてこなければならないことになる．

6. リピートRNA結合蛋白質の登場

Timchenkoらは，DNAのCTGリピートまたはmRNAのCUGリピートに結合する分子としてCELFファミリーに属するCUG-BP(CUG-binding protein)を単離した．CUG-BPは*in situ* hybridizationによって確かに，長いリピートをもつDMPK mRNAに結合して核に存在することがわかり，これが何らかの機能にかかわっていることを示唆した[7]．続いて，CUG-BPは，心筋トロポニンT(心伝導障害)，インスリン受容体(耐糖能)，塩素チャネル(ミオトニア)，タウ(精神遅滞)，マイオチューブラリン(筋分化)などのmRNAのスプライシング活性に作用

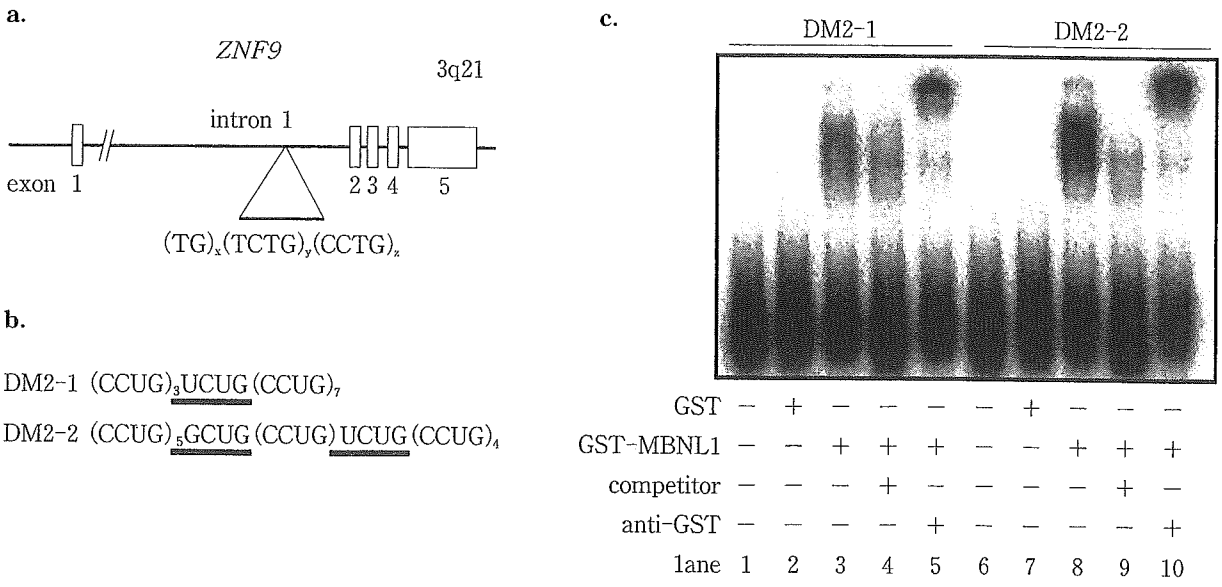

図2 DM2の責任遺伝子 *ZNF9*

a: DM2は，第3染色体長腕に存在する*ZNF9*遺伝子の，第1イントロンにあるCCTGリピートの伸長で起こる．

b: DM2の患者にみられるリピート2種類

c: ゲル・リターデーション・アッセイ．GST-MBNL1は，2人の患者のRNA配列に結合することがわかる．この結合は標識なしのcompetitorの添加で弱まり，結合物の移動度は抗GSTの添加で変化する．

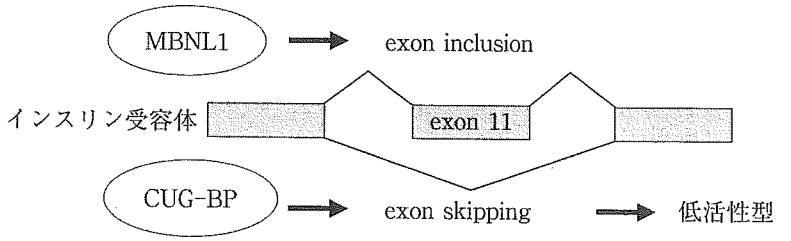

図3 インスリン受容体のスプライシング

CUG-BPは，インスリン受容体のエキソン11をスキップさせ，低活性の受容体を作らせるが，MBNL1にはそのような活性はない．

することが幾人もの研究者から明らかにされ，CUG-BP説が急激に頭をもたげてきた．インスリン受容体のスプライシング異常(エキソン11のスキッピング)によって，機能の低下した非筋型バリアントが作られ，これがインスリン非感受性を引き起こす(**図3**)．また筋特異的塩素チャネルClC-1のスプライシング異常が膜の過剰興奮を引き起こし，ミオトニアに導く．CUG-BPはこれらの鍵となる因子である．

しかし著者らは，この説に疑問をもった．著者らは，RNA結合能を調べる酵母three hybrid法という系をもっている[8]．これは，蛋白質-蛋白質相互作用をみるtwo hybrid法の変型で，RNA-蛋白質相互作用を調べるものである．これでCUG-BPとCUGリピートの相互作用を調べてみると，結合能力は非常に弱く，長さ依存性もない．結局CUG-BPは，CUGリピートよりもUGというジヌクレオチドリピートに強固に結合することがわかった(**表1**)．

それでは生体内でCUGリピートに結合する因子は何であろうか．

現在のところ，いくつものRNAリピート結合蛋白質が報告されているが，著者らはMBNL1(muscleblind-like 1: EXPとも呼ばれ